Sound Transmission through Gaps in Pressure Release Barriers.

P.A Cotterill[ac], C.P Walker[a], R. Harter[a] and I.D. Abrahams[b].

a) Thales Underwater Systems Ltd., Dolphin House, Bird Hall Lane, Cheadle Heath, Stockport, SK3 0XB.
b) School of Mathematics, University of Manchester, Oxford Road, Manchester, M13 9PL.
c) P.A. Cotterill is partially funded under a Royal Society Industry Fellowship.

The problem of predicting the level of sound transmitted through a gap in a pressure release barrier is considered. The Kirchhoff-Helmholtz equation is used to derive a boundary integral expression for the unknown scattered field, whose derivative satisfies a boundary condition on the gap. The resulting singular integral equation is solved for the scattered field across the gap. Once the gap pressure is known, the scattered field at any location can be calculated. Its near-field and far-field behaviour is considered with respect to directivity and frequency dependence.

1. Introduction

Reflecting sound barriers are commonly used to reduce the noise radiated into an acoustic medium by a vibrating structure. The barrier may be acoustically hard or soft, the choice mainly depending upon the properties of the acoustic medium. For example in-air, acoustically hard or "rigid" barriers can be very effective at reflecting unwanted sound, whilst the high acoustic impedance of water makes it difficult to achieve a rigid barrier. Hence it is more common to use acoustically soft or "pressure release" barriers in underwater acoustics. It is seldom possible to maintain a continuous acoustic barrier and the question arises as to the impact of gaps upon the barrier's effectiveness. Here we consider a two dimensional problem in which an infinite planar barrier is insonified by an acoustic plane wave upon one side. A small gap in the barrier allows sound to pass through and we wish to determine the far-field source strength of the gap and how this scales with frequency and gap width. In particular, we consider a pressure-release barrier as this gives rise to a singular boundary integral equation for the scattered field that is hard to solve by the usual discretisation methods. Rather, it is solved using the method of Achenbach [1] in which an exact Green's function for the problem is written as a Fourier integral, and the unknown gap pressure is expressed as the sum of an infinite series of Chebyshev polynomials whose coefficients are determined by applying a boundary condition. This gives rise to an infinite set of simultaneous equations in these unknown coefficients. In practice, the Chebyshev polynomial series can be truncated after a suitable number of terms that depends upon the ratio of the gap length to the acoustic wavelength. The resulting finite set of simultaneous equations is easily solved numerically, allowing the gap-pressure and far-field source level to be determined. At low and high frequencies, approximate analytic solutions exist, and these are used to validate the exact Chebyshev series representation. These approximate solutions show that to leading order, the pressure radiated through the gap at low frequencies scales as the ratio of gap length to acoustic wavelength raised to the power of 3/2, whilst at high frequencies the power law scaling is 1/2. Numerical results are presented for both gap pressure and far-field source levels. Finally an extension to multiple gaps is illustrated by way of a specific example.

2. The Boundary Parameter Problem

The problem under consideration is illustrated in figure 1. An infinite pressure-release barrier, located at $y = 0$, contains a small gap of width $2a$ centred at the origin. A plane harmonic wave of angular frequency ω, and acoustic wavenumber k_0, is incident upon the barrier from the half-space Ω_1 in $y < 0$. The incident wave is denoted,

$$P_i e^{-i\omega t} = P_0 e^{i\{k_0(x\sin\theta + y\cos\theta) - \omega t\}}.$$

It gives rise to both specular and diffuse reflections in Ω_1, denoted $P_r e^{-i\omega t}$ and

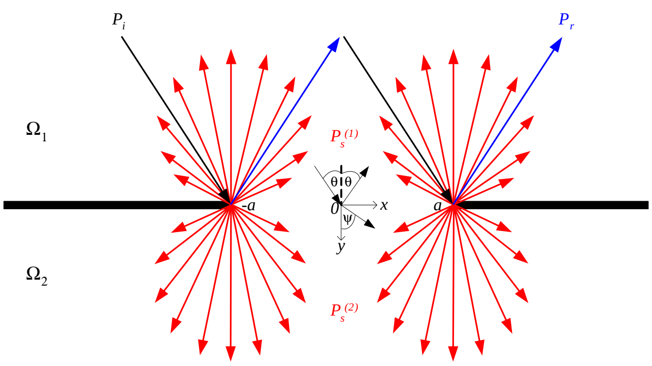

Figure 1: The pressure fields

$P_s^{(1)}e^{-i\omega t}$ respectively, and to a diffuse transmitted field in the half-space Ω_2 in $y>0$, denoted $P_s^{(2)}e^{-i\omega t}$. The total pressure $Pe^{-i\omega t}$ is denoted $P_1e^{-i\omega t}$ in Ω_1, and $P_2e^{-i\omega t}$ in Ω_2, where

$$P_1 = P_i + P_r + P_s^{(1)},$$
$$P_2 = P_s^{(2)}.$$

$P_r = -P_0 e^{ik_0(x\sin\theta - y\cos\theta)}$ is the complex amplitude of the reflected field from a continuous pressure release surface located in $y=0$, thus $P_i + P_r = 0$ on $y=0$. All fields share a common time dependence of $e^{-i\omega t}$, which is omitted from now on for brevity of notation. $P_s^{(1)}$ and $P_s^{(2)}$ are referred to collectively as the scattered field. The total pressure vanishes on the surface of the barrier, and is continuous across the gap, as is its normal derivative $\partial P/\partial y$. This leads to the following boundary parameter problem for the scattered field:

$$\begin{aligned} P_s^{(1)} &= P_s^{(2)} = 0, \qquad |x| > a, y = 0, \\ P_s^{(1)} &= P_s^{(2)} \;= f(x), \quad |x| \le a, y = 0, \end{aligned} \tag{1}$$

$$\frac{\partial P_s^{(2)}}{\partial y} - \frac{\partial P_s^{(1)}}{\partial y} = \frac{\partial}{\partial y}(P_i + P_r) \;= 2h(x), \qquad |x| \le a, y = 0, \tag{2}$$

where $f(x)$ denotes the unknown gap pressure of the scattered field and $h(x) = iP_0 k_0 \cos\theta \, e^{ik_0 x\sin\theta}$.

3. The Boundary Integral Formulation

The Kirchhoff-Helmholtz equation, which is easily derived from Green's second identity [2], equates the harmonic pressure P, within some source-free volume V, to a boundary integral on the enclosing surface ∂V, viz

$$P(\underline{x}') = \iint_{\partial V} \left\{ P(\underline{x}) \frac{\partial G}{\partial n}(\underline{x};\underline{x}') - G(\underline{x};\underline{x}') \frac{\partial P}{\partial n}(\underline{x}) \right\} dS,$$

where $\partial P/\partial n = \underline{\nabla P} \cdot \underline{n}$ is the spatial derivative of P in the direction of the outward pointing unit normal $\underline{n}$ to the surface element dS, and G is a Green's function that satisfies the inhomogeneous Helmholtz equation for a point source at $\underline{x}' = (x', y')$, viz

$$\left(\nabla^2 + k_0^2\right) G(\underline{x};\underline{x}') = \delta(\underline{x} - \underline{x}'). \tag{3}$$

Applying the Kirchhoff-Helmholtz equation to the scattered field of the two-dimensional half-space Ω_1 in figure 1 gives

$$\begin{aligned} P_s^{(1)}(\underline{x}_1) = &\int_{-\infty}^{\infty} \left\{ P_s^{(1)}(x,0) \frac{\partial G}{\partial y}(x,0;\underline{x}_1) - G(x,0;\underline{x}_1) \frac{\partial P_s^{(1)}}{\partial y}(x,0) \right\} dx \\ &+ \int_{\partial S_\infty} \left\{ P_s^{(1)}(\underline{x}) \frac{\partial G}{\partial n}(\underline{x};\underline{x}_1) - G(\underline{x};\underline{x}_1) \frac{\partial P_s^{(1)}}{\partial n}(\underline{x}) \right\} dS, \qquad \underline{x}_1 \in \Omega_1, \end{aligned}$$

where ∂S_∞ is an infinite arc, connecting $x = +\infty$ and $x = -\infty$ in Ω_1 (see figure 2).

However $P_s^{(1)}$ and G are required to satisfy the Somerfeld-Watson radiation condition, which ensures that the integrand vanishes along ∂S_∞. G can be any solution of the inhomogeneous Helmholtz equation, we choose a Dirichlet form, denoted G_D, that vanishes on $y=0$. When this form is used in conjunction with the boundary conditions (1) for $P_s^{(1)}$, the equation above reduces to

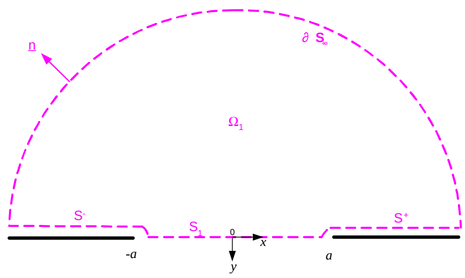

Figure 2. The integration contour

$$P_s^{(1)}(\underline{x}_1)=\int_{-a}^{a} f(x)\frac{\partial G_D}{\partial y}(x,0;\underline{x}_1)dx, \qquad \underline{x}_1\in\Omega_1. \tag{4}$$

Similarly, in Ω_2

$$P_s^{(2)}(\underline{x}_2)=-\int_{-a}^{a} f(x)\frac{\partial G_D}{\partial y}(x,0;\underline{x}_2)dx, \qquad \underline{x}_2\in\Omega_2, \tag{5}$$

where the negative sign comes from the outward normal being in the -*y* direction for Ω_2. Finally, taking the derivatives of (4) and (5) with respect to their *y*-coordinates, and applying the boundary condition (2) for the derivative of the scattered pressure gives

$$\int_{-a}^{a} f(x)\frac{\partial^2 G_D}{\partial y'\partial y}(x,0;x',0)dx=-h(x'), \qquad |x'|\le a. \tag{6}$$

4. Achenbach's Method

Solving (6) for $f(x)$, allows the scattered field to be determined via equations (4) and (5). But owing to the nature of the Green's function, (6) is a singular integral equation. It is solved here using a method described by Achenbach [1], in which the Green's function is represented by a Fourier integral transform, and $f(x)$ is expanded as an infinite series of Chebyshev polynomials, viz

$$f(x)=2\sum_{j=1}^{\infty} A_j\frac{C_j(x/a)}{j}, \tag{7}$$

where

$$C_j(\xi)=\begin{cases}\cos(j\sin^{-1}\xi), & j \text{ odd}\\ i\sin(j\sin^{-1}\xi), & j \text{ even.}\end{cases}$$

To obtain the Green's function we use the method of images in the boundary $y=0$ and write

$$G_D(\underline{x};\underline{x}')=G_F(\underline{x};x',y')-G_F(\underline{x};x',-y'),$$

where G_F is a free-field Green's function for an unbounded medium. For our two dimensional problem $G_F(\underline{x},\underline{x}')=\frac{-i}{4}H_0^{(1)}(k_0R)$, where $H_0^{(1)}$ is a Hankel function of the first kind, and $R=\sqrt{(x-x')^2+(y-y')^2}$. Its Fourier integral representation is best derived directly from the inhomogeneous Helmholtz equation (3), by taking the Fourier transform in (x,y) to obtain the spectral Green's function in (k_x,k_y), and then taking the inverse Fourier transform in k_y whilst requiring the solution to contain only outwardly propagating/decaying waves, whence

$$G_D=\frac{-i}{4\pi}\int_{-\infty}^{\infty} e^{ik(x'-x)}\left\{\frac{e^{i\gamma|y-y'|}-e^{i\gamma|y+y'|}}{\gamma}\right\}dk, \tag{8}$$

where $\gamma=\sqrt{k_0^2-k^2}$ is defined to be positive when real and the integration path in k is taken above the branch point at $-k_0$ and below the branch point at $+k_0$. Thus we find

$$\frac{\partial^2 G_D}{\partial y'\partial y}(x,0;x',0)=\frac{-i}{2\pi}\int_{-\infty}^{\infty}\gamma\, e^{ik(x'-x)}dk. \tag{9}$$

We now substitute (7) and (9) into (6) and make use of the identity [1]

$$\int_{-a}^{a} C_m(x/a)e^{-ikx}dx=\frac{m\pi}{k}J_m(ka) \tag{10}$$

to carry out the integral in x. Both sides of the resulting equation are then multiplied by $C_m^*(x'/a)$, where * denotes complex conjugation, and integrated over x' between the limits of $\pm a$ to finally obtain

$$\sum_{j=1}^{\infty} Q_{mj} A_j = b_m\,, \qquad m = 1,2,\ldots,\infty, \tag{11}$$

where

$$Q_{mj} = \begin{cases} \int_0^{\infty} t^{-2}(t^2-1)^{1/2} J_m(\varepsilon t) J_j(\varepsilon t)\,dt, & m+j \text{ even}, \\ 0, & m+j \text{ odd}, \end{cases} \tag{12}$$

$$b_m = \begin{cases} \dfrac{-iP_0\varepsilon\delta_{1m}}{2}, & \theta = 0, \\ -iP_0 \cot\theta\, J_m(\varepsilon\sin\theta)\,, & \theta \neq 0, \end{cases} \tag{13}$$

and $\varepsilon = k_0 a$. In practice (11) can be truncated, with good convergence, for maximum values of j and m of order ε. The coefficients A_j then give the gap pressure directly via (7). To obtain the scattered field at other locations we return to (4) and (5), making use of (7) and (8). However, we note from (8) that $\dfrac{\partial G_D}{\partial y}(x,0;x',-y') = -\dfrac{\partial G_D}{\partial y}(x,0;x',y'),\ y' > 0,$ and hence

$$P_s^{(1)}(x',-y') = P_s^{(2)}(x',y') = -\int_{-a}^{a} f(x)\frac{\partial G_D}{\partial y}(x,0;x',y')\,dx, \quad y' \geq 0\,. \tag{14}$$

In the next section we present results for the gap pressure, and the far-field source level that can be derived from (14), (7), (8) and (10) using the method of steepest descent. The derivation is omitted here but the far-field source level at an angle ψ to the normal is found to be

$$SL_{ff} = \lim_{R\to\infty}\left(\sqrt{\frac{R}{a}}\left|P_s(R,\psi)\right|\right) \approx \sqrt{2\pi\varepsilon}\,\cos\psi\,\left|g(\varepsilon\sin\psi)\right|, \tag{15}$$

with

$$g(\varphi) = \sum_{j=1}^{\infty} A_j \varphi^{-1} J_j(\varphi),$$

where the source level is defined to be the magnitude of the scattered pressure in the limit $R \to \infty$, scaled back to a distance of $R = a$, using the cylindrical spreading law applicable to 2D problems.

5. Results

It is clear from the analysis above that the dependence of the scattered fields upon frequency is through the non-dimensional parameter $\varepsilon = k_0 a$, and the spatial dependence of the gap pressure is through the non-dimensional coordinate $\xi = x/a$, in which the gap extends over the region $|\xi| \leq 1$. Results are presented below, in terms of these dimensionless parameters, for a unit incident field of $P_0 = 1$.

5.1. Validation

Figure 3 compares the gap pressure and far-field source level obtained using the Achenbach method, at a very low frequency of $\varepsilon \sim 0.04$ and an angle of incidence of 45°, with the leading order term of an approximate analytic solution that is valid for $\varepsilon << 1$. The derivation of that solution is not given here but it is obtained from a perturbation expansion in ε, which leads to a boundary parameter problem for each order that can be solved using conformal mapping techniques. The leading order gap pressure is found to be $P_{gap} = -i\varepsilon\cos\theta\sqrt{1-\xi^2}$, and the leading order far-field source level is

$$SL_{ff} = \varepsilon^{3/2}\sqrt{\pi/8}\,\cos\theta\cos\psi. \tag{16}$$

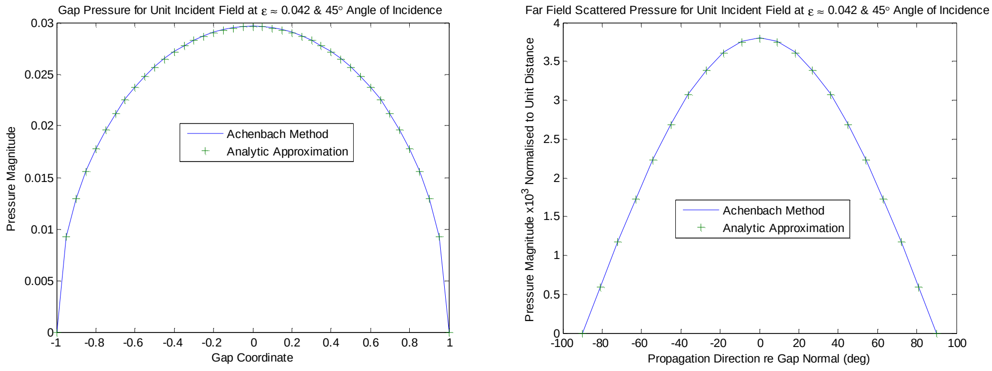

Figure 3. Comparison of the Achenbach solution with a low frequency analytic approximation. Gap pressure (left); far-field source level (right)

At high frequencies an approximate analytic solution may be obtained using the Wiener-Hopf method [3, 4]. Figure 4 compares the gap pressure obtained from the Achenbach method, with the analytic solution given in §5.6 of [3], for $\varepsilon \sim 25$ and an angle of incidence of 45°.

The agreement between the Achenbach series solution and the approximate analytic methods is exceedingly good at both large and small ε, as shown by figures 3 and 4, giving confidence in the results obtained using the former.

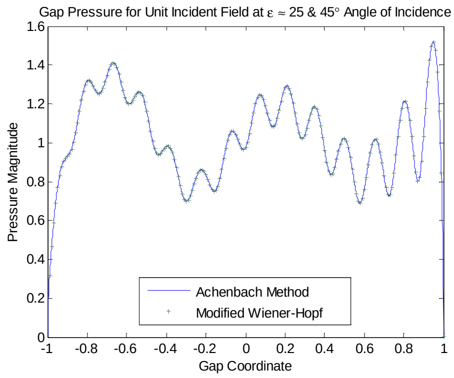

Figure 4. Comparison of the Achenbach solution with a high frequency analytic approximation.

5.2. Directivity

Figure 5 shows the far-field source-level as a function of angle, measured from the normal, for two angles of incidence: 0° and 45°. The left hand plot is at low frequency, $\varepsilon \sim 0.4$, and apart from overall normalisation, the two curves are very similar in shape as expected from the low frequency asymptotic analysis described above; the low frequency directional dependence of $\cos\psi$ is essentially that of a point source in a pressure release baffle. The magnitude of the response varies with the incidence angle as $\cos\theta$, because the scattered field is proportional to the normal derivative of $P_i + P_r$, through (6). The right hand plot is at higher frequency, $\varepsilon \sim 25$, and shows quite different behaviour. The gap is now several wavelengths wide, and this imparts a directional characteristic to the scattered field with a main lobe and multiple side-lobes. As ε increases, the direction of the transmitted field becomes more and more confined to the angle of incidence, whilst the diffuse reflected field becomes confined to the direction of specular reflection. The width of the main lobe reduces as ε increases. The magnitude of the response again varies with the incidence angle as $\cos\theta$.

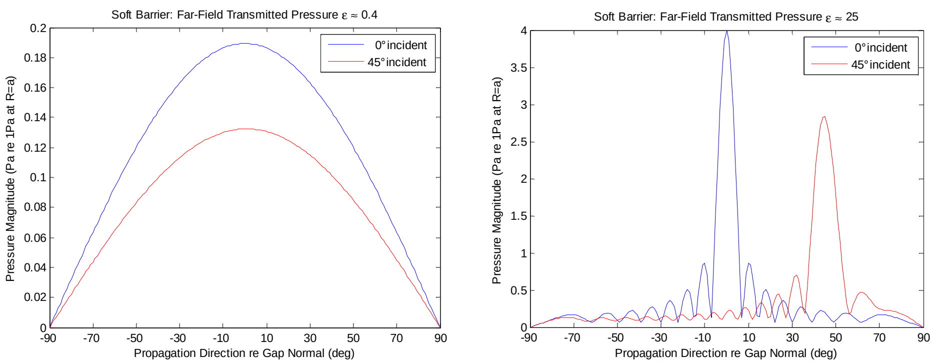

Figure 5. Low frequency directivity (left); high frequency directivity (right)

5.3. Frequency Dependence

The red and blue curves in Figure 6 denote far-field source level spectra for the field transmitted through a single gap in the same direction as the angle of incidence. Angles of incidence of 0º and 45º are shown for a non-dimensional frequency range $0.042 \le \varepsilon \le 42$. Each curve exhibits an $O(\varepsilon^{3/2})$ dependence for $\varepsilon \le 1$ and an $O(\varepsilon^{1/2})$ dependence for $\varepsilon \ge 4$. This is consistent with (16) at low frequencies, and with the behaviour of the leading order term of the Wiener-Hopf solution [3] at high frequencies. The change in the gradient of the curves, from $\varepsilon^{3/2}$ to $\varepsilon^{1/2}$, occurs approximately at a frequency when half a wavelength fits across the gap. Furthermore, the figure shows that at low frequencies, the far-field sound level for a 45º angle of incidence is a factor of 0.5 times that at 0º, which is consistent with (16) through the term $\cos\theta\cos\psi$. At high frequencies the difference is less, about 0.7, which is consistent with the results found in the previous section. The larger reduction in level at low frequencies is due the field being greatest in a direction normal to the gap, irrespective of the angle of incidence, giving rise to an additional dependency on $\cos\psi$ if the field is calculated away from the normal. These directional properties were illustrated in figure 5.

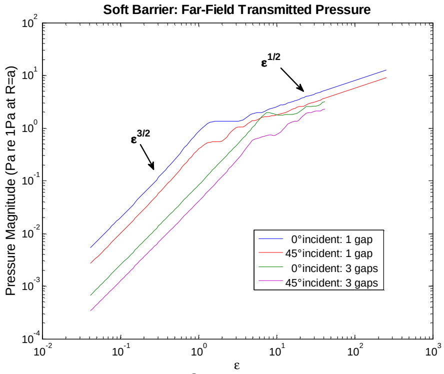

Figure 6. Far-field sound level spectra

5.4. Multiple Gaps

Figure 6 also shows the corresponding far-field source level spectra (denoted by the green and purple curves) transmitted through $M = 3$ identical gaps. The dimensional length $2a$ is now defined to be the distance that just encompasses all three gaps. Each gap is of length $l = 2a\delta,\ \delta < M^{-1}$. In figure 6, $\delta = 1/5$ and the gaps are equally spaced, thus the gap separation is also l. In comparison with a single gap of length $2a$, their effect is to reduce far-field sound levels by a factor of ~0.12 at low frequencies and ~0.62 at high frequencies. The former is almost exactly the same as the value of $M\delta^2 = 0.12$ that can be derived from the low frequency approximation given by (16), for M locally non-interacting gaps whose far-field pressures are coherent.

6. Concluding Remarks

Using the method of Achenbach, an exact solution has been derived for the field scattered by a gap in a pressure release barrier. In this solution the gap pressure is expanded as an infinite series of Chebyshev polynomials, which in practice can be truncated at order $\varepsilon = k_0 a$. Given the coefficients of the Chebyshev polynomials, the gap pressure is obtained directly by summing the Chebyshev polynomial series. The pressure at any other location is expressed as a boundary integral, over the gap, of the product of the gap pressure and the derivative of a Green's function. This boundary integral may be converted, via Fourier decomposition of the Green's function, to a sum of wavenumber integrals involving Bessel functions that can be evaluated numerically. A particularly simple form is found for the far-field limit, which just involves a sum over Bessel functions. The methodology, which has been validated against approximate analytic solutions, is readily adapted to more complex geometries; as an example, multiple gaps in a pressure release barrier have been modelled. In future we will apply Achenbach's method to the more realistic geometries found in industrial applications for which analytic solutions are extremely difficult, if not impossible, to obtain.

7. References

1. *Reflection and Transmission of Scalar Waves by a Periodic Array of Screens,* J.D. Achenbach and Z.L. Li, Wave Motion 8 (1986) 225-234, North-Holland.
2. *Mathematical Methods in the Physical Sciences,* M.L. Boas, John Wiley & Sons, Inc., 1966.
3. *Methods Based on the Wiener-Hopf Technique for the Solution of Partial Differential Equations,* B. Noble, Chelsea Publishing Co., New York.
4. *Scattering of Sound by Large Finite Geometries,* I.D. Abrahams, IMA Journal of Applied Mathematics 29 (1982), 79-97.